The Side Chain of Aspartic Acid 69 Dictates the Folding Mechanism of *Bacillus subtilis* HPr[†]

Jason P. Schmittschmitt and J. Martin Scholtz*

Department of Medical Biochemistry and Genetics and Department of Biochemistry and Biophysics, Center for Advanced Biomolecular Research, Texas A&M University, College Station, Texas 77843-1114

Received September 25, 2003; Revised Manuscript Received December 9, 2003

ABSTRACT: Many small, single-domain proteins show equilibrium and kinetic folding mechanisms that appear to be adequately described as two state. The two-state model makes several predictions that can be tested experimentally. First, the conformational stability determined at or extrapolated to a set of reference conditions should be independent of the measurement method (thermal or solvent denaturation or hydrogen exchange). Second, model-independent measures of the cardinal thermodynamic parameters (T_m, ΔH) as determined from direct calorimetric means should be identical to those determined from the two-state analysis of thermal unfolding data. Third, the ratio of the kinetic folding and unfolding rate constants should be equal to K_{eq} determined from an equilibrium measurement under the same conditions. Here, we show that the wild-type HPr protein from *Bacillus subtilis* does not meet all of these criteria under our standard conditions. However, if we replace the side chain of Asp69, or add moderate concentrations of salt, we find excellent two-state behavior in both equilibrium and kinetic folding. Thus, for this protein and possibly others, very subtle changes in the primary structure or in the solution conditions can dramatically alter the relative stabilities of the native intermediate, and unfolded ensembles can cause an observable change in the nature of the folding mechanism.

A hallmark feature of many small monomeric proteins is that they obey a simple, reversible two-state folding reaction (*1*):

$$F \Leftrightarrow U \tag{1}$$

where only the folded (F) and unfolded (U) conformations are populated and no intermediates can be detected at equilibrium. The two-state mechanism greatly simplifies the analysis of the folding transition and allows for simple methods to measure the Gibbs free energy change (ΔG) for the folding reaction, often referred to as the conformational stability of the protein (*2*):

$$K_{eq} = [U]/[F] \tag{2}$$

$$\Delta G = -RT \ln K_{eq} \tag{3}$$

Since a protein exists almost exclusively in the folded conformation under native conditions, a common method to measure the conformational stability is to perturb the relative populations of the F and U by alterations in temperature or solvent composition, measure ΔG using eqs 2 and 3 through the unfolding transition region, and extrapolate ΔG to native conditions. The two traditional methods employed to perturb the equilibrium, and therefore provide a measure of K_{eq}, are thermal and solvent denaturation. The details of both have been described in detail (*2*) and are presented briefly below.

An alternative technique used to measure the conformational stability of a protein is the hydrogen exchange (HX)[1] experiment as monitored by NMR. In this experiment, a protonated protein is placed in D_2O, and the amide protons are allowed to exchange with deteurons from the solvent over a period of time. The amide exchange rate is dependent upon the experimental conditions, the intrinsic exchange rate of the amide, and its environment in the protein. The mechanism of exchange can be described by

$$(N-H\cdots O{=}C)_{cl} \underset{k_{cl}}{\overset{k_{op}}{\Leftrightarrow}} (N-H)_{op} \xrightarrow{k_{rc}} N-D \tag{4}$$

where k_{op} and k_{cl} are the rate constants for the structural opening and closing reaction and k_{rc} is the rate constant for exchange from the open state (*3*−*5*). Under the EX2 conditions, where $k_{cl} \gg k_{rc}$, the rate constant for exchange is $k_{ex} = (k_{op}/k_{cl})k_{rc} = K_{op}k_{rc}$, where K_{op} is the equilibrium

[†] This work was supported by grants from the National Institutes of Health (GM 52483) and the Robert A. Welch Foundation (BE-1281). The NMR instrumentation was obtained, in part, with funds from the National Science Foundation (DBI-9970232).

* To whom correspondence should be addressed at 440 Reynolds Medical Building, Texas A&M University, 1114 TAMU, College Station, TX 77843-1114. Phone: 979-845-0828. Fax: 979-847-9481. E-mail: jm-scholtz@tamu.edu.

[1] Abbreviations: GdnHCl, guanidine hydrochloride; HX, hydrogen exchange; wt, the wild-type HPr protein; D69A*, the double mutant D69A + G49E; ΔG_{UDC}, conformational stability determined from the analysis of urea denaturation curves; ΔG_{GDC}, conformational stability determined from the analysis of guanidine hydrochloride denaturation curves; ΔG_{HX}, conformational stability determined from hydrogen exchange; ΔG_U, general term for the conformational stability determined from equilibrium measurements; DSC, differential scanning calorimetry; CD, circular dichroism; pH*, direct pH reading in D_2O.

10.1021/bi0357412 CCC: $27.50
Published on Web 01/15/2004

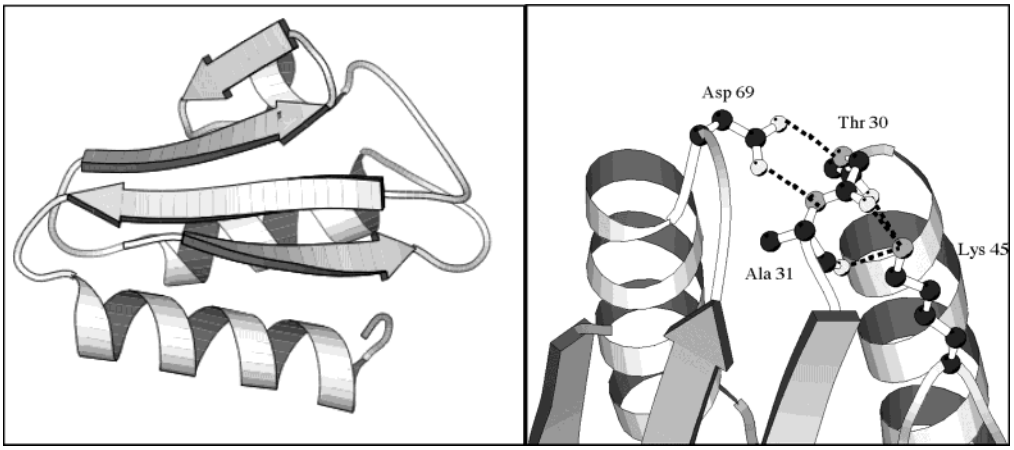

FIGURE 1: Ribbon drawing of the entire HPr protein from *B. subtilus* (left panel) and detailed view of the hydrogen bond network associated with Asp69 (right panel). Asp69 links the loops shown on the left-hand side of the right panel. The figures were made with MOLSCRIPT (*40*).

constant for structural opening, and the free energy change for structural opening, ΔG_{HX}, for each measurable amide group can be given by

$$\Delta G_{HX} = -RT \ln(k_{ex}/k_{rc}) \quad (5)$$

This technique can measure ΔG_{HX} under fully native conditions, thus obviating the need for any extrapolations from high temperature or denaturant concentration. While the EX2 mechanism is two state at the level of each exchangeable site (open or closed as described by eq 4), it makes no assumptions about the nature of the overall conformational transition of the protein.

The two-state model makes several predictions that can be tested experimentally (*2*). First, the unfolding transition for a given type of denaturation experiment (thermal or solvent) must be independent of the probe used to monitor the relative populations of F and U. Second, values of ΔG and the other thermodynamic parameters must also be independent of the method used to unfold the protein.

Another method to test for the two-state nature of the folding transition is to compare equilibrium and kinetic ΔG and m values. A number of small, single-domain proteins appear to fold and unfold in a single step without detectable intermediates (*6*). But often, even if the equilibrium transition is adequately described as two state, the kinetic folding mechanism shows transient kinetic intermediates (*7*). By investigating the denaturant dependence to the observed kinetic rate constants, the folding and unfolding rate constants in the absence of denaturant and their associated m values can be determined (see below). For a simple two-state mechanism, the ratio of the extrapolated rate constants, k_f^{water} and k_u^{water}, should equal the equilibrium constant determined from the stability measurements. In addition, the kinetic m values should add to the m value determined from an equilibrium denaturation experiment.

The focus of the current study is the HPr protein from *Bacillus subtilis*, a key protein in the PEP-dependent phosphotransferase system in bacteria (*8*). The structure has been determined by crystallographic (*9*) and NMR techniques (*10*). The fold, which is common for all the HPr proteins studied to date, is that of a mixed $\alpha + \beta$ protein (Figure 1). The HPr proteins have been extensively studied as models for the protein folding and stability (*11*−*15*). Here, we present a comparison of the equilibrium and kinetic folding for the HPr protein from *B. subtilis* and a key variant, D69A. From an inspection of all the known HPr structures, Asp69 appears to participate in a key tertiary interaction that links two critical loops in the structure (Figure 1). Our preliminary studies revealed that the side chain of Asp69 is an important contributor to the overall stability of the HPr protein. We also observed that ΔG_{HX} is substantially larger than ΔG_U, as determined by either solvent or thermal denaturation for the wt HPr protein but not for variants that removed the side chain of Asp69. To discover the reasons for these observations, we performed a detailed thermodynamic and kinetic comparison of the wt HPr protein and the variant, D69A*. Here, we show that the wild-type (wt) protein in the absence of salt does not fold by a simple two-state mechanism; however, removing a single charged side chain (Asp69) or adding NaCl is enough to convert the folding transition for HPr back to a simple two-state reaction.

MATERIALS AND METHODS

Design and Production of B. subtilis HPr Variants. In this study, we employed two variants of the HPr protein derived from *B. subtilis*. The proteins were produced in an *Escherichia coli* strain lacking the endogenous *E. coli* HPr protein (*ptsH*$^-$), and the expression was under the control of the natural *ptsH* promotor. The expressed proteins lack the first Met residue of the natural *B. subtilus* HPr protein. The G49E variant is a stabilized version of the HPr protein (*16*), similar to the K49E variant of the *E. coli* HPr protein (*17*). Asp69 is involved in a key hydrogen bond network that is critical to the stability of the HPr protein (*18*). The D69A + G49E double mutant, which we call D69A*, removes this key side chain in the background of the stabilizing variant, G49E. The identity of all of the proteins was confirmed by high-resolution mass spectrometry.

The ^{15}N-labeled wt protein was prepared as described previously (*16*). For the D69A* variant, the *E. coli* cells harboring the plasmid for HPr were grown in the same manner as wt except that the large-scale growth was performed at 42 °C. The higher temperature was used to promote inclusion body formation. After overnight growth, the cells were harvested and combined into one pellet by centrifugation and washed with 10 mM Tris and 1 mM

EDTA, pH 8.0. The cells were lysed and centrifuged, and the pellet was resuspended in 2 M GdnHCl to resolubilize the protein and centrifuged again to remove any remaining insoluble material. The supernatant was dialyzed against three 4 L changes of 10 mM Tris and 1 mM EDTA, pH 8.0, buffer, and any insoluble material was removed by centrifugation. The remaining supernatant was desalted with a G-50 column equilibrated with 50 mM ammonium bicarbonate.

Urea and GdnHCl Denaturation Studies. The conformational stability of the HPr variants was determined using urea or GdnHCl denaturation as monitored by circular dichroism spectroscopy with an Aviv 62DS or Aviv SF 202 spectropolarimeter. In some cases, the urea (Nacalai Tesque) was deuterated by several cycles of lyophilization from D_2O. The stock solutions of urea were prepared fresh daily. Protein stock solutions were prepared in H_2O or D_2O in 50 mM sodium phosphate at pH 7.0. For experiments with GdnHCl, the same stock solution was used for all experiments. Urea and GdnHCl concentrations were determined using refractive index measurements (*19*). A thorough explanation of the methods used to analyze the solvent denaturation curves has been previously described (*2*, *12*). Briefly, the unfolding curves were fit by an equation derived from the linear extrapolation method (LEM) (*2*, *20*):

$$\theta_{obs} = \{([\theta_N] + a_N[D]) + ([\theta_D] + a_D[D])\exp[m([D] - C_m)/RT]\}/\{1 + \exp[m([D] - C_m)/RT]\} \quad (6)$$

where θ_{obs} is the spectroscopic signal of the unfolding reaction, [D] is the molar denaturant concentration, a_N and a_D are the denaturant dependence, and $[\theta_N]$ and $[\theta_D]$ are the *y*-intercepts of the pre- and posttransition baselines, respectively. The parameter *m* is a measure of the dependence of the ΔG on denaturant concentration, and C_m is the midpoint of the denaturation curve. The conformational stability in water (ΔG_{UDC} or ΔG_{GDC}) is obtained by multiplying the C_m and the *m* values.

Thermal Denaturation Studies. Thermal denaturation was also monitored by CD, as described for the solvent denaturation experiments. The resulting data were fit by a modified version of the van't Hoff equation:

$$\theta_{obs} = \left[(N_0 + a_N T) + (D_0 + a_D T)^* \exp\left(\frac{\Delta H_{vH}}{R}\left(\frac{1}{T_g} - \frac{1}{T}\right)\right)\right] \Big/ \left[1 + \exp\left(\frac{\Delta H_{vH}}{RT}\left(\frac{1}{T_g} - \frac{1}{T}\right)\right)\right] \quad (7)$$

where θ_{obs} is the spectroscopic signal monitoring the unfolding reaction, a_N and a_D represent the unfolding dependence of the pre- and posttransition baselines, and N_0 and D_0 are the values of the folded and unfolded baselines at 0 °C. The fit also resolves the thermal midpoint T_g of the unfolding process and the associated van't Hoff enthalpy change, ΔH_{vH}.

Differential Scanning Calorimetry. All measurements were performed with a Microcal VP-DSC calorimeter. The usual scan rate was 60 °C/h over a temperature range of 5−100 °C, but no scan rate dependence was observed from 30 to 90 °C/h. Two consecutive scans were performed to assess reversibility. HPr solutions, ranging from 25 to 150 μM, were dialyzed overnight at 4 °C against buffer containing 10 mM potassium phosphate, pH 7.0, and the specified concentration of NaCl. Dialyzed protein and buffer were used for the sample and reference cells, respectively. Experimental data were corrected for small inconsistencies between the two cells by subtracting the buffer−buffer baseline scan prior to data analysis. After normalizing for protein concentration, the progress curves were analyzed by a two-state fit model using the Origin software package.

Kinetic Folding Studies. The stopped-flow CD measurements at 222 nm were performed on an Aviv 202 SF CD at 25 °C. HPr (≈3 mg/mL) in denaturant was rapidly mixed to give an 11-fold dilution in 10 mM potassium phosphate at pH 7.0. Unfolding kinetic reactions were the average of 10−20 reactions and fit by either a single or double exponential function using KaleidaGraph. The folding reactions were performed by diluting HPr (≈3 mg/mL) in buffered urea 11-fold into 10 mM potassium phosphate, pH 7.0, to initiate refolding. Kinetic measurements were performed 10−20 times under identical conditions, averaged, and fit by

$$\ln k_{obs} = \ln[k_f^{water}\exp(-m_f[D]/RT) + k_u^{water}\exp(m_u[D]/RT)] \quad (8)$$

Kinetic Data Analysis. For a two-state folding mechanism, eq 8 was fit to the observed rate constants as a function of urea to resolve the *m* values and rate constants for the unfolding and folding reactions in the absence of denaturant. For those reactions that exhibited a substantial burst phase in the refolding reaction, we assumed a preequilibrium where the amplitudes of the refolding phase represent the populations of the intermediate in the folding mechanism. Thus, the stability associated with this event (ΔG_{UI}), as represented by the change in amplitude with urea concentration, can be determined using eq 6. The observed kinetic phase was fit by eq 8 to afford a measure of the stability of the second refolding phase (ΔG_{IN}).

Hydrogen Exchange (HX) by NMR Experiments. Samples for the HX experiments consisted of 10−20 mg of ^{15}N-labeled protein in D_2O with sodium acetate-d_3 (pH* 5.5) as the buffer. To prepare the samples, the lyophilized protein was first dissolved in H_2O with the same salt and buffer composition as the desired NMR sample. The protein was then rapidly transferred to D_2O using a small spin column equilibrated in deuterated buffers as described previously (*21*). The exchange process was monitored by recording a series of two-dimensional ^{1}H−^{15}N HSQC spectra at regular intervals over the course of the exchange process. These were acquired on a Varian Unity Plus or Varian Inova NMR spectrometer operating at 500 or 600 MHz proton frequencies. All spectra were obtained using a ^{1}H spectral width of 6410 Hz, the ^{15}N spectral width was 1800 Hz, with a decoupler offset of 1043 Hz, and the HSQC data sets contained 192 × 1K complex points. Pulsed field gradients were used for water suppression in these experiments. HSQC experiments were processed, and peak picking was performed using the nmrPipe/nmrDraw processing and visualization software (*22*).

RESULTS

Thermal and Solvent Denaturation Studies. The far-UV circular dichroism (CD) spectra for the folded conformations of the wt and D69A* protein are identical and show typical

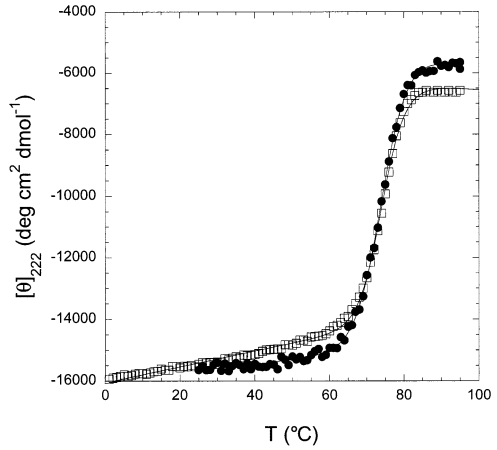

FIGURE 2: Thermal unfolding curves, as monitored by CD at 222 nm, for wt (□) and D69A* (●). The curves through the data represent the fit of eq 7 to the data, and the parameters from the fits are given in Table 1.

$\alpha + \beta$ secondary structure features with minima at 222 and 206 nm (data not shown). Figure 2 shows typical thermal unfolding curves, as monitored by CD, for wt HPr and the D69A* variant. The curves show a single unfolding transition that appears very sigmoidal and cooperative, consistent with a two-state unfolding transition. One interesting feature is the pronounced slope in the pretransition baseline for the wt HPr protein, whereas for D69A*, it is very nearly flat. The cardinal thermodynamic parameters derived from the CD-monitored thermal unfolding curves for the proteins are shown in Table 1.

As we have shown previously (*11*, *12*, *16*, *17*), the urea denaturation curves of HPr and variants show a single unfolding transition and appear two state and cooperative. We also used GdnHCl as a denaturant (data not shown), and the resulting C_m, m, and ΔG_{GDC} values are also given in Table 1. For the wt protein, the ΔG values determined from GdnHCl denaturation do not agree with the values determined using urea as the denaturant. This is not unexpected because GdnHCl is a salt, and often ΔG values from urea and GdnHCl denaturation experiments do not agree (*2*, *23*). Interestingly, the ΔG values determined from GdnHCl and urea denaturation studies agree for D69A* (Table 1).

To compare ΔG values determined from thermal and solvent denaturation experiments and to provide an estimate of ΔC_p, the method of Pace and Laurents (*24*) was used to construct the stability curves (*25*) for the HPr variants (*11*, *12*) by combining the CD-monitored thermal unfolding curves and the urea denaturation curves at various temperatures (Figure 3). The combined data sets were fit by a modified Gibbs−Helmholtz equation, assuming a temperature-independent ΔC_p:

$$\Delta G(T) = \Delta H_g(1 - T/T_g) - \Delta C_p[(T_g - T) + T \ln(T/T_g)] \quad (9)$$

The thermodynamic parameters resolved from this fit are shown in Table 1, and the stability curves in Figure 3 are constructed from these parameters. The fit is very good, suggesting that CD-monitored thermal and urea denaturation experiments are providing identical measures for ΔG under a wide variety of solution conditions, consistent with a two-state folding/unfolding reaction.

Table 1: Thermodynamic Parameters for the Stability of the HPr Proteins[a]

	wt	D69A*	wt + salt	wt (D_2O)	D69A* (D_2O)	wt + salt (D_2O)
TDC[b]						
T_g (°C)	74.2	69.7	68.5			
ΔH_{vH} (kcal mol^{-1})	73.5	71.2	62.0			
ΔC_p (kcal mol^{-1} K^{-1})	1.45	1.59	ND			
ΔG(25 °C) (kcal mol^{-1})	5.1	4.4	ND			
UDC[c]						
m (kcal mol^{-1} M^{-1})	1.0	1.1	1.1	1.0	1.1	1.1
C_m (M)	4.9	3.9	3.4	4.9	3.9	3.4
ΔG_{UDC} (kcal mol^{-1})	4.9	4.2	3.8	4.8	4.2	3.7
GDC[d]						
m (kcal mol^{-1} M^{-1})	2.4	2.4	ND			
C_m (M)	1.3	1.8	ND			
ΔG_{GDC} (kcal mol^{-1})	3.2	4.3	ND			
DSC[e]						
T_g (°C)	74.9	70.0	68.5			
ΔH_{cal} (kcal mol^{-1})	52.7[g]	71.5	63.3			
$\Delta H_{vH}/\Delta H_{cal}$	1.39	1.00	0.98			
HX[f]						
ΔG_{HX} (kcal mol^{-1})				6.8	4.9	3.7
kinetic data[g]						
ΔG_{UI} (kcal mol^{-1})	2.0			2.0		
ΔG_{IN} (kcal mol^{-1})	4.9			5.0		
ΔG_{UN} (kcal mol^{-1})	6.9	4.6	3.9	7.0	4.7	ND

[a] The errors on the T_m values are ±0.2 °C, ΔH values ±2.5 kcal mol^{-1}, ΔC_p ±0.1 kcal mol^{-1} K^{-1}, m values ±0.1 kcal mol^{-1} M^{-1}, and ΔG ±0.1−0.2 kcal mol^{-1}. [b] From the analysis of thermal denaturation curves (Figure 2), as monitored by CD at pH 7.0. The ΔC_p and ΔG(25 °C) values are from the fit of eq 9 to the combined data from thermal and urea unfolding studies as shown in Figure 3. [b] From the analysis of urea denaturation curves, as monitored by CD at 25 °C, pH 7.0. The values in D_2O were collected at pH* 5.5 to match the conditions used in the HX experiment. [c] From the analysis of GdnHCl denaturation curves, as monitored by CD at 25 °C, pH 7.0. [d] Results from the differential scanning calorimetry studies on the HPr proteins at pH 7.0 (Figure 5). [e] Results from the HX data collected at 25 °C, pH* 5.5 in D_2O. The values were obtained by averaging the three largest residue-specific ΔG_{HX} values. [f] Derived from the kinetic data shown in Table 2 at 25 °C, pH 7.0. [g] This represents only the major transition observed in the DSC endotherm in Figure 5 and does not include any aspect of the pretransition region at low temperature.

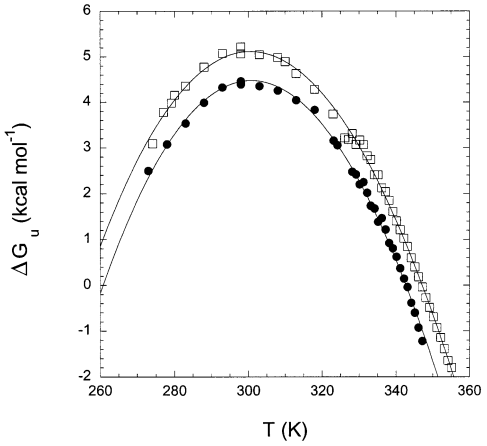

FIGURE 3: Stability curves for the wt (□) and D69A* (●) HPr proteins. The data points at the lower temperatures are derived from urea denaturation curves while the higher temperature points are from thermal unfolding experiments. The curves through the data are a fit of eq 8 to the data, and the parameters derived from the fit are shown in Table 1.

Equilibrium Hydrogen Exchange (HX) Experiments. As discussed above, an alternative method to measure the

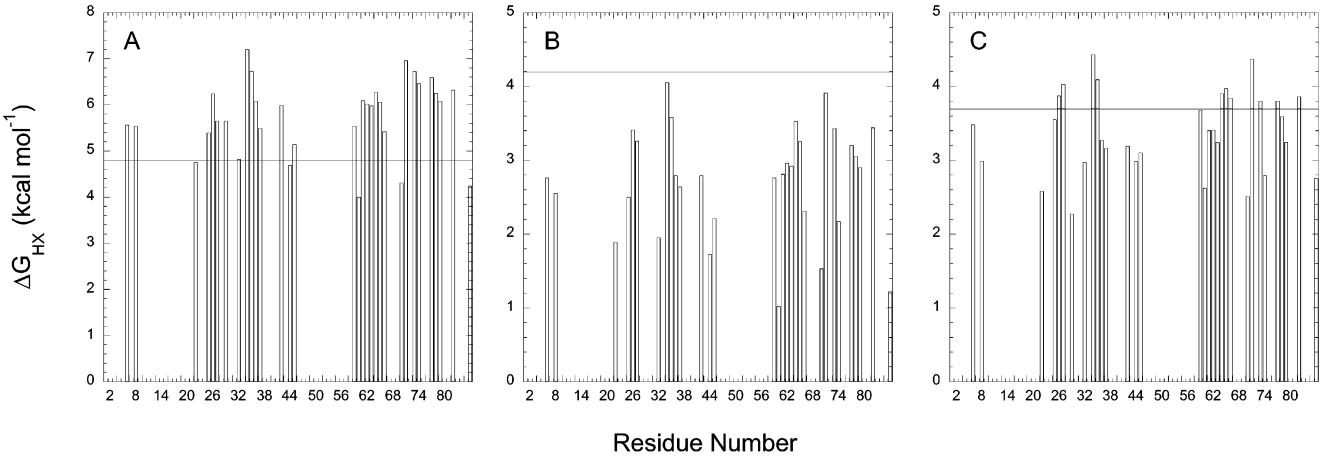

FIGURE 4: Residue-specific stabilities (ΔG_{HX}) as determined from hydrogen exchange experiments for (A) wt, (B) D69A*, and (C) wt in 0.25 M NaCl. The ΔG_{HX} values were determined from the observed rates of exchange as described in the text. The horizontal lines represent the global stability as determined from urea denaturation curves performed in D_2O to match the conditions used in the hydrogen exchange experiment.

conformational stability of a protein is the HX experiment (see ref *21* and references cited therein). For the wt protein, we were able to measure the exchange rates for 32 non-overlapping amide protons by following their peak intensities in $^1H-^{15}N$ HSQC spectra over time. Figure 4A shows the ΔG_{HX} values for the amide protons calculated from eq 5. The horizontal solid line at 4.8 kcal mol^{-1} is the ΔG_{UDC} value from urea denaturation in D_2O under the same conditions employed in the HX experiment. There are a number of residues that have stabilities greater than the ΔG_{UDC} value. Since the correction for Xaa−Pro isomerization (*21*, *26*) is very small for HPr (≈0.1 kcal mol^{-1}), our results show a substantial amount of "super protection". When the same HX experiment is performed on the D69A* variant (Figure 4B) or on the wt protein in the presence of 0.25 M NaCl (Figure 4C), we find good agreement between ΔG_{HX} and ΔG_{UDC}. Our results show that the addition of salt or the replacement of the side chain of Asp69 abolishes super protection.

Differential Scanning Calorimetry. To further test the validity of the two-state mechanism for HPr, differential scanning calorimetry (DSC) was used to analyze the thermal unfolding of the HPr proteins (Figure 5). The results were compared to the model-dependent values measured by the CD unfolding curves. A feature that is apparent in the DSC endotherms for the wt protein in the absence of salt is the slope in the pretransition region. This slope is absent in the D69A*, reminiscent of the similar behavior observed in the CD-monitored thermal unfolding curves. This result is independent of the protein concentration (data not shown), indicating it is not likely the result of protein aggregation. The analysis of the DSC endotherms provides estimates of ΔH_{cal} and T_g, and the data are shown in Table 1. The ΔH_{vH} values from the CD thermal denaturations curves are compared with the ΔH_{cal} values to assess the validity of the two-state model for these proteins. For the wt protein, $\Delta H_{vH}/\Delta H_{cal} = 1.4$ in the absence of salt and 0.98 in 0.25 M NaCl. In contrast, D69A* shows perfect agreement between ΔH_{vH} and ΔH_{cal}. The thermal denaturation of HPr in the absence of salt does not appear to follow a two-state folding mechanism, but by adding 0.25 M salt or removing the side chain of Asp69, the thermal unfolding of HPr appears to fold by a two-state folding mechanism.

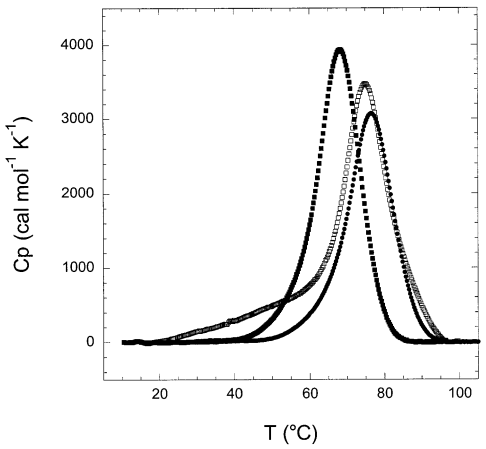

FIGURE 5: Representative differential scanning calorimetry (DSC) traces for wt (□), D69A* (●), and wt in 0.25 M NaCl (■) at pH 7.0 recorded as described in the text. The parameters that describe these traces are shown in Table 1.

Folding Kinetics. Stopped-flow CD was used to follow the kinetics of the folding and unfolding of the HPr variants, wt and D69A*, at 222 nm, 25 °C. The refolding of the wt protein shows a large decrease in the CD signal within the dead time of the instrument (≈5 ms) (data not shown). This burst phase is followed by a slower reaction that fits well to a single exponential (k_{obs} = 19 s^{-1} at [urea]$_{final}$ of 0.6 M), indicating that wt HPr refolding is at least a biphasic process such as

$$\mathrm{U} \underset{k_{IU}}{\overset{k_{UI}}{\leftrightarrow}} \mathrm{I} \underset{k_{NI}}{\overset{k_{IN}}{\leftrightarrow}} \mathrm{N} \qquad (10)$$

Such biphasic kinetics suggests that a kinetic intermediate (I) is populated early in the refolding of the wt HPr protein. (Two alternative mechanisms, parallel folding and one in which there is an off-pathway intermediate, are discussed below.) On the other hand, D69A* refolds and fits well to a single exponential process. The observed refolding phase of D69A* accounts for ≥90% of the total amplitude, suggesting that it follows a two-state folding mechanism.

The burst phase intermediate for the wt protein forms within the dead time of the instrument (≈5 ms), indicating that the apparent rate constant for the formation of the burst

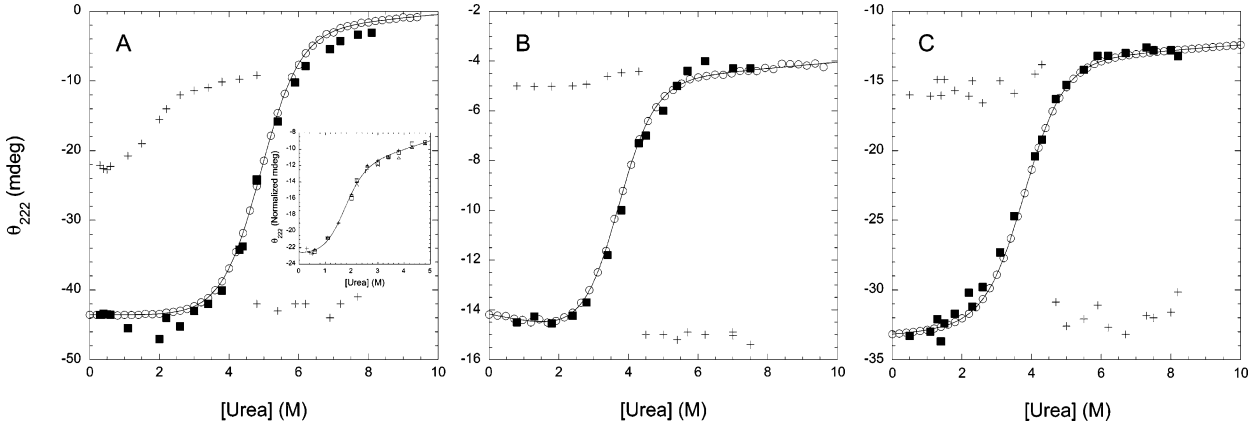

FIGURE 6: Urea dependence to the final amplitudes from the kinetic folding experiments for (A) wt HPr, (B) D69A*, and (C) wt HPr in 0.25 M NaCl. The crosses (+) represent the initial signals of the observable kinetic phase and the filled squares (■) represent the final signals. The open circles depict the equilibrium urea denaturation curve. The insert to (A) shows the urea dependence to the initial burst phase signal at three different protein concentrations (20, 30, and 40 μM). The curves through the data represent fits of eq 6, and the resolved parameters are given in Table 1.

phase must be >200 s^{-1}. Since the k_{obs} of the slow, observable phase (19 s^{-1} at 0.6 M urea) is an order of magnitude slower than the burst phase, we can treat the burst phase as a preequilibrium between the unfolded and intermediate states (*27*, *28*). The change in the population of the intermediate, as reflected in the amplitude of the burst phase as a function of the final urea concentration, can therefore be used to estimate the stability of the intermediate (Figure 6). Assuming a two-state transition between the U and I states, the thermodynamic stability of the folding intermediate can be determined using eq 6. The conformational stability of the U to I is $\Delta G_{UI} = 2.0$ kcal mol^{-1} ($C_m = 2.0$ M; $m = 1.0$ kcal mol^{-1} M^{-1}; see Table 1). The stability of the kinetic intermediate is modest but makes an important contribution to the overall stability of the wt HPr protein.

The kinetics of refolding/unfolding was examined over a wide range of urea concentrations for both wt and the D69A* variant. As noted above, the refolding of the wt protein shows a burst phase intermediate; however, D69A* does not. All of the unfolding experiments for both proteins can be fit well by a single exponential function, indicating the lack of intermediates in the unfolding reaction. Figure 7 shows the combined kinetic data for the observable phases for the wt protein, the D69A* variant, and wt in 0.25 M NaCl. The dependence of ln k_{obs} on the urea concentration has the typical "chevron" shape, with the left arm of the curve dominated by the refolding rate constant and the right arm of the curve dominated by the unfolding rate constant. The k_{obs} data were fit using a simple two-state model (eq 8) that describes the transition from I to N for wt and U to N for D69A* (Table 2). We also measured the folding and unfolding kinetics in D_2O to directly compare the kinetics to the HX results. The D_2O results are also shown in Tables 1 and 2.

The conformational stability, as determined by the kinetic rate constants, can be compared to the ΔG values determined from equilibrium measurements (Table 1). For D69A*, there is excellent agreement between the kinetic and equilibrium ΔG values. For wt, the observed kinetic rate constants (I to N) also agree with the CD-monitored equilibrium measurements of ΔG when the stability of the burst phase intermediate is not included. A further test is provided by a comparison of the kinetic and equilibrium m values. For D69A*, the kinetic and equilibrium m values agree (Tables 1 and 2),

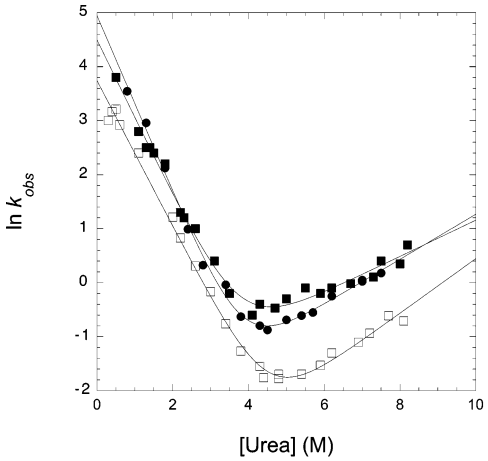

FIGURE 7: Urea dependence of the kinetic folding and unfolding rate constants for the wt HPr protein in no salt (□) and in 0.25 M NaCl (■) and for the D69A* (●) variant. The curves through the data represent a fit of eq 8 to the data, and the parameters describing the fit are shown in Table 2.

but for wt, agreement is only seen when the burst phase is ignored.

The compactness of the transition state, relative to the folded state, can be represented by the β_T value ($\beta_T = m_f/m_{eq}$). This value reflects the placement of the transition state on the folding reaction coordinate based upon compactness, where $\beta_T = 0$ represents a transition state with the same solvent-accessible surface area as the unfolded state whereas a $\beta_T = 1$ represents a transition state which is as compact as the native state. The β_T value is 0.72 for wt HPr and 0.80 for D69A*, suggesting that the transition state is highly compact in both variants.

Characterization of the Kinetic Intermediate in Wild-Type HPr. For the wt HPr protein, there is good agreement between the equilibrium and kinetically determined ΔG and m values only when the burst phase is ignored, suggesting that the burst phase might be an artifact of the stopped-flow experiment caused by either aggregation or solvent reorganization (*29*, *30*). Previous studies have shown that transient protein aggregation can cause deviations from linearity in the plot of logarithm of refolding versus denaturant concentration as well as the appearance of a burst phase (*29*, *30*).

Table 2: Kinetic Parameters for the HPr Proteins[a]

	wt	D69A*	wt + salt	wt (D_2O)	D69A* (D_2O)
k_f (s^{-1})	42	140	90	79	84
k_u (s^{-1})	0.0099	0.055	0.12	0.016	0.031
m_f (kcal mol^{-1} M^{-1})	0.79	0.96	0.85	0.76	0.85
m_u (kcal mol^{-1} M^{-1})	0.31	0.24	0.20	0.25	0.32
m (kcal mol^{-1} M^{-1})	1.10	1.20	1.05	1.01	1.17
C_m (M)	4.4	3.8	3.8	4.9	4.0
ΔG_{UI} (kcal mol^{-1})	2.0			2.0	
ΔG_{IN} (kcal mol^{-1})	4.9			5.0	
ΔG_{UN} (kcal mol^{-1})	6.9	4.6	3.9	7.0	4.7

[a] The kinetic rate constants and the associated m_u and m_f values are from a fit of eq 8 to the urea dependence of the observed rate constants as shown in Figure 7. The m value is the sum of the resolved kinetic m values, and the C_m represents the urea concentration where $k_f = k_u$. The ΔG_{UI} values for wt were determined from a fit of eq 6 to the amplitudes of the burst phase (Figure 6), and the ΔG_{IN} values are determined from the observed rate constants for folding and unfolding. The ΔG_{UN} values for wt in H_2O and D_2O are the sums of the ΔG_{UI} and ΔG_{IN} values while the ΔG_{UN} for D69A* is calculated from the observed rate constants. The errors on each parameter are approximately k_f ±3, k_u ±0.003, m_f ±0.04, m_u ±0.06, C_m ±0.07, m ±0.06, and ΔG ±0.2.

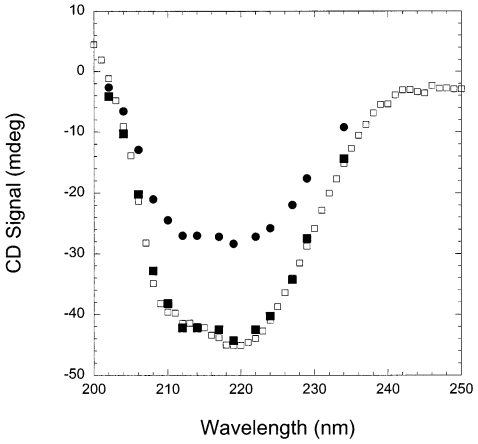

FIGURE 8: Reconstruction of the CD spectra for the burst phase (■) and final amplitudes (●) derived from the kinetic folding experiments compared with the spectrum for the folded wt protein (□). All of the experiments were performed at 25 °C, pH 7.0.

Therefore, we investigated the dependence of protein concentration on the folding kinetics for wt HPr. As seen in the insert to Figure 6A, there is no change in the urea dependence to the amplitude of the burst phase as the protein concentration is varied. Also, we did not observe a change in any of the observable rate constants, suggesting that protein aggregation is not occurring, at least over the concentration range investigated here.

To further investigate the nature of the burst phase intermediate, we reconstructed the CD spectrum from the burst phase amplitudes measured at different wavelengths (Figure 8). The large CD signal and spectral properties indicate that this early intermediate has a significant amount of secondary structure. Furthermore, the spectrum of this intermediate appears to be very similar to that of the fully native state. The combined amplitudes for the burst and observable phases are also shown in Figure 8 and are identical to the spectrum for the native protein. As expected for a protein that shows a two-state folding mechanism, the spectrum for the D69A* variant reconstructed from the final amplitudes of the observable kinetic traces is identical to the spectrum of the fully folded form (data not shown).

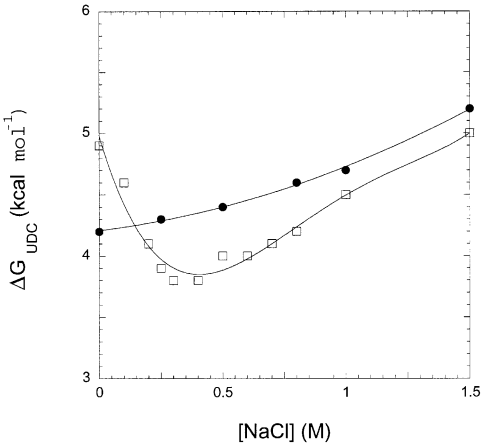

FIGURE 9: NaCl dependence to the conformational stability of the wt (□) and D69A* (●) HPr proteins. The ΔG_{UDC} values were determined from the analysis of urea denaturation curves performed at pH 7.0, 25 °C, in the indicated concentration of NaCl. The curves through the data have no theoretical significance.

Salt Effects on the Stability and Folding of HPr. The ΔG calculated from GdnHCl equilibrium denaturation (ΔG_{GDC}) of wt HPr are not equivalent to ΔG_{UDC} calculated from urea denaturations (see Table 1). The ΔG calculated from urea and GdmCl are equivalent, however, for D69A*. We explored this further by monitoring the effects of NaCl on equilibrium stability for wt and D69A* (Figure 9). There is a large decrease in the stability for the wt HPr protein between 0 and 0.25 M NaCl followed by a gradual increase in stability up to 1.5 M NaCl. D69A* does not show, however, a decrease in stability at low concentrations of salt, but rather a gradual increase, matching the stability change in the wt protein. Similarly in the HX experiment, as noted above, the presence of 0.25 M NaCl abolishes the super protection in the wt protein (Figure 4). We also performed a kinetic folding study on wt HPr in 0.25 M NaCl to determine if the presence or stability of the kinetic intermediate observed in the refolding of the wt protein is altered as we add salt. In the presence of salt, the burst phase intermediate is not observed, and the kinetics adhere to a simple two-state mechanism. Thus, we have two ways to induce wt HPr to obey two-state folding: adding salt and removing the side chain of Asp69.

DISCUSSION

It has long been suggested that the HX technique can be used to determine the conformational stability of a protein (*31*−*33*), and recently it has been shown that conformational stability determined by HX (ΔG_{HX}) is identical to the values measured by more conventional equilibrium unfolding studies (ΔG_U) using either thermal or solvent denaturation, provided the differences in Xaa−Pro isomerization and solvent (H_2O vs D_2O) are included (*21*, *34*). This conclusion supports the notion that, for some residues, the protein must globally unfold for exchange to occur.

In a previous analysis, Huyghues-Despointes et al. (*34*) concluded that, with one exception, the corrected $\Delta G_{HX} = \Delta G_U$ within the limits of the error on the two measurements (defined such that $\Delta G_{HX} - \Delta G_U < 1$ kcal mol^{-1}). There was one protein where ΔG_{HX} was substantially larger than

ΔG_U; the src SH3 domain (*35*) showed a 1.4 kcal mol^{-1} difference (6.1 vs 4.7 kcal mol^{-1}, respectively, for ΔG_{HX} and ΔG_U). This so-called super protection, which we also define as $\Delta G_{HX} - \Delta G_U > 1$ kcal mol^{-1}, has now also been observed in two other recent studies (*36*, *37*) on the prion proteins (PrP), where ΔG_{HX} is larger than ΔG_U by $\approx$1.5−3 kcal mol^{-1}, respectively, for the Syrian hamster and mouse forms of the PrP protein.

There are several reasons why ΔG_{HX} might be larger than ΔG_U even after the correction for the differences in the *cis*/*trans* isomerization of Xaa−Pro bonds has been applied and the measurements of ΔG_{HX} and ΔG_U have been obtained in identical solvents (H_2O vs D_2O) as described previously (*34*). For example, in the determination of ΔG_U, there are several criteria that must be met: (1) The equilibrium unfolding refolding must be reversible and exhibit two-state (or a finite number of states) behavior. (2) In the analysis of solvent denaturation studies, one assumes that the linear extrapolation method (LEM) applies, and likewise for thermal unfolding experiments, one must have accurate values for ΔC_p in order to extrapolate stability measurements from higher to ambient temperatures. In the analysis of HX measurements, there are additional considerations: (1) Does the EX2 mechanism adequately describe the exchange process such that eq 5 can be used to determine ΔG_{HX}? (2) Do the peptide-based values for k_{rc} apply to the unfolded (i.e., exchange competent) form of the protein?

One of the primary motivations for this study was to explore why ΔG_{HX} was substantially larger than ΔG_U, as determined by either solvent or thermal denaturation, for the wt HPr protein from *B. subtilis*. To discover the origin of this super protection, we performed a detailed thermodynamic and kinetic comparison of the wt HPr protein and a key variant, D69A*. Since the D69A mutation is very destabilizing, we constructed the D69A variant in the background of the stabilizing variant G49E (*16*). The double mutant D69A* thus shows very nearly the same stability as the wt HPr protein using thermal and urea denaturation (Figure 3 and Table 1).

The principal result in this study is that the folding of the wt HPr protein does not adhere to a two-state mechanism in the absence of salt, and thus the equilibrium thermal or solvent denaturation curves underestimate the true conformational stability. The HX data, on the other hand, do report on the overall conformational stability. The full analysis of the kinetic data also agrees with the HX data and thus represents the true conformational stability of HPr. Furthermore, the lack of agreement of the enthalpy change determined from DSC (ΔH_{cal}) with the model-dependent ΔH_{vH} from TDC suggests that the two-state model is invalid. In retrospect, we had a hint of some potential deviation from two-state behavior from an inspection of the pretransition baselines in the thermal unfolding curves (Figure 2) and the DSC endotherms (Figure 5) for wt HPr; however, the origins of slopes in the baselines of thermal unfolding curves are not known and difficult to predict and interpret (*2*).

The kinetic data provide the most convincing evidence for non-two-state behavior. The refolding data for the wt HPr protein show two phases: a burst phase followed by a slower phase that can be measured by conventional stopped-flow techniques. The rate constants for the slower observable phase change in the typical fashion, providing the chevron behavior for the folding and unfolding reactions (Figure 7). It should be noted that while curved chevron plots are often observed for proteins that fold via intermediates, the absence of detectable "rollover" does not mean that intermediates are not present. Rollover in the refolding limb of the chevron plot can be seen when the rate constant for the observable refolding phase is approximately the same as the rate constant of the unfolding event for the phase that cannot be observed directly. Since the observable rate constants for HPr folding are small for proteins of this size (*6*), it is quite possible that the extrapolated rate constant for the missing phase is much larger, and thus we do not observe rollover even though an intermediate is present. In our case, ΔG calculated from the extrapolated rate constants agrees with that determined from equilibrium urea or thermal unfolding (Table 1). In addition, the kinetic *m* values also agree with the equilibrium *m* value determined from the urea denaturation measurements (Table 2). Together, these results suggest that the same conformational transition is being monitored by the equilibrium denaturation experiments and the observable folding and unfolding reactions in the kinetic experiments.

The refolding reaction of the wt HPr protein also shows a very fast "burst" phase which occurs within the dead time of our instrument ($\approx$5 ms). We have elected to model the three-state character with a model that places the intermediate "on pathway", but the alternative "off pathway" or "parallel pathway" mechanisms could also work (*7*). Since we cannot measure the rate constants associated with this first transition in refolding, we are not able to distinguish between the potential models. Under these circumstances, these fundamentally distinct mechanisms become indistinguishable, and we are forced to treat this first transition with a model that depicts a preequilibrium between U and I (eq 10). Although we cannot measure the kinetic constants for this fast refolding phase, we can measure the amplitude of the phase as a function of the final urea concentration. These amplitudes change in the expected sigmoidal fashion as a function of the urea concentration (Figure 6), and therefore we can calculate the difference in free energy for this transition (Table 1). The resulting ΔG, 2 kcal mol^{-1}, accounts for the super protection observed when comparing the HX and equilibrium urea denaturation experiments (Table 1). Therefore, we conclude that the full kinetic data, including the burst phase, and the HX data represent the true conformational stability of the wt HPr protein in the absence of added salt.

In contrast, all of the available evidence suggests that the D69A* variant and the wt HPr protein in the presence of moderate concentrations of NaCl adhere to a two-state folding mechanism. There is no super protection in the HX experiment, the ratio of ΔH_{vH} to ΔH_{cal} is unity, and there is not a detectable burst phase intermediate in the refolding reaction. Furthermore, all of the estimates of ΔG and the measurements of the *m* values agree, as expected for a two-state folding mechanism.

The related HPr protein from *E. coli* has been shown to follow a two-state kinetic folding mechanism using GdnHCl as the denaturant (*13*), although recent studies on Trp variants of the *E. coli* HPr protein suggest deviations from a strict two-state mechanism (*14*, *15*). We are in the process of providing a full description of the folding mechanism of the *E. coli* HPr protein and key variants to compare with the *B.*

subtilis HPr results here. Further studies will also be necessary to determine if the D69A mutation itself is responsible for the change in folding mechanism and/or the change in the relative stabilities of intermediates or if any destabilized variant can cause a switch from three- to two-state folding, as has been found for other proteins including ubiquitin (*38*) and protein G (*39*).

ACKNOWLEDGMENT

We thank Drs. Ronald Peterson, Beatrice Huyghues-Despointes, and David Schell for assistance in collecting the HX data and for helpful comments, Abbas Razvi for assistance with the DSC, and the laboratory of Dr. C. Robert Matthews for assistance with preliminary kinetic folding studies.

REFERENCES

1. Lumry, R., and Biltonen, R. (1966) Validity of the "two-state" hypothesis for conformational transitions of proteins, *Biopolymers 4*, 917−944.
2. Pace, C. N., and Scholtz, J. M. (1997) in *Protein Structure: A Practical Approach* (Creighton, T. E., Ed.) pp 299−321, IRL Press, Oxford.
3. Hvidt, A., and Nielsen, S. O. (1966) Hydrogen exchange in proteins, *Adv. Protein Chem. 21*, 287−386.
4. Bai, Y., Milne, J. S., Mayne, L., and Englander, S. W. (1993) Primary structure effects on peptide group hydrogen exchange, *Proteins: Struct., Funct., Genet. 17*, 75−86.
5. Bai, Y., Milne, J. S., Mayne, L., and Englander, S. W. (1994) Protein stability parameters measured by hydrogen exchange, *Proteins: Struct., Funct., Genet. 20*, 4−14.
6. Jackson, S. E. (1998) How do small single-domain proteins fold?, *Folding Des. 3*, R81−R91.
7. Baldwin, R. L. (1996) On-pathway versus off-pathway folding intermediates, *Folding Des. 1*, R1−R8.
8. Herzberg, O., and Klevit, R. (1994) Unraveling a bacterial hexose transport pathway, *Curr. Opin. Struct. Biol. 4*, 814−822.
9. Herzberg, O., Reddy, P., Sutrina, S., Saier, M., Reizer, J., and Kapadia, G. (1992) Structure of the histidine-containing phosphocarrier protein HPr from *Bacillus subtilis* at 2.0 Å resolution, *Proc. Natl. Acad. Sci. U.S.A. 89*, 2499−2503.
10. Wittekind, M., Rajagopal, P., Branchini, B. R., Reizer, J., Saier, M. J., and Klevit, R. E. (1992) Solution structure of the phosphocarrier protein HPr from *Bacillus subtilis* by two-dimensional NMR spectroscopy, *Protein Sci. 1*, 1363−1376.
11. Scholtz, J. M. (1995) Conformational stability of HPr: the histidine-containing phosphocarrier protein from *Bacillus subtilis*, *Protein Sci. 4*, 35−43.
12. Nicholson, E. M., and Scholtz, J. M. (1996) Conformational stability of the *Escherichia coli* HPr protein: Test of the linear extrapolation method and a thermodynamic characterization of cold denaturation, *Biochemistry 35*, 11369−11378.
13. van Nuland, N. A., Meijberg, W., Warner, J., Forge, V., Scheek, R. M., Robillard, G. T., and Dobson, C. M. (1998) Slow cooperative folding of a small globular protein HPr, *Biochemistry 37*, 622−637.
14. Canet, D., Lyon, C. E., Scheek, R. M., Robillard, G. T., Dobson, C. M., Hore, P. J., and van Nuland, N. A. (2003) Rapid formation of non-native contacts during the folding of HPr revealed by real-time photo-CIDNP NMR and stopped-flow fluorescence experiments, *J. Mol. Biol. 330*, 397−407.
15. Azuaga, A. I., Canet, D., Smeenk, G., Berends, R., Titgemeijer, F., Duurkens, R., Mateo, P. L., Scheek, R. M., Robillard, G. T., Dobson, C. M., and van Nuland, N. A. (2003) Characterization of single-tryptophan mutants of histidine-containing phosphocarrier protein: evidence for local rearrangements during folding from high concentrations of denaturant, *Biochemistry 42*, 4883−4895.
16. Nicholson, E. M., Peterson, R. W., and Scholtz, J. M. (2002) A partially buried site in homologous HPr proteins is not optimized for stability, *J. Mol. Biol. 321*, 355−362.
17. Peterson, R. W., Nicholson, E. M., Thapar, R., Klevit, R. E., and Scholtz, J. M. (1999) Increased helix and protein stability through the introduction of a new tertiary hydrogen bond, *J. Mol. Biol. 286*, 1609−1619.
18. Hammen, P. K., Scholtz, J. M., Anderson, J. W., Waygood, E. B., and Klevit, R. E. (1995) Investigation of a side-chain-side-chain hydrogen bond by mutagenesis, thermodynamics, and NMR spectroscopy, *Protein Sci. 4*, 936−944.
19. Pace, C. N. (1986) Determination and analysis of urea and guanidine hydrochloride denaturation curves, *Methods Enzymol. 131*, 266−280.
20. Santoro, M. M., and Bolen, D. W. (1988) Unfolding free energy changes determined by the linear extrapolation method. 1. Unfolding of phenylmethanesulfonyl α-chymotrypsin using different denaturants, *Biochemistry 27*, 8063−8068.
21. Huyghues-Despointes, B. M., Pace, C. N., Englander, S. W., and Scholtz, J. M. (2001) in *Methods in Molecular Biology* (Murphy, K. P., Ed.) pp 69−92, Humana Press, Totowa, NJ.
22. Delaglio, F., Grzesiek, S., Vuister, G., Zhu, G., Pfeifer, J., and Bax, A. (1995) NMRPipe: a multidimensional spectral processing system based on UNIX Pipes, *J. Biomol. NMR 6*, 277−293.
23. Makhatadze, G. I. (1999) Thermodynamics of protein interactions with urea and guanidinium hydrochloride, *J. Phys. Chem. 103*, 4781−4785.
24. Pace, C. N., and Laurents, D. V. (1989) A new method for determining the heat capacity change for protein folding, *Biochemistry 28*, 2520−2525.
25. Becktel, W. J., and Schellman, J. A. (1987) Protein stability curves, *Biopolymers 26*, 1859−1877.
26. Reimer, U., Scherer, G., Drewello, M., Kruber, S., Schutkowski, M., and Fischer, G. (1998) Side-chain effects on peptidyl-prolyl cis/trans isomerisation, *J. Mol. Biol. 279*, 449−460.
27. Kuwajima, K., Yamaya, H., Miwa, S., Sugai, S., and Nagamura, T. (1987) Rapid formation of secondary structure framework in protein folding studied by stopped-flow circular dichroism, *FEBS Lett. 221*, 115−118.
28. Raschke, T. M., and Marqusee, S. (1997) The kinetic folding intermediate of ribonuclease H resembles the acid molten globule and partially unfolded molecules detected under native conditions, *Nat. Struct. Biol. 4*, 298−304.
29. Silow, M., and Oliveberg, M. (1997) Transient aggregates in protein folding are easily mistaken for folding intermediates, *Proc. Natl. Acad. Sci. U.S.A. 94*, 6084−6086.
30. Ferguson, N., Capaldi, A. P., James, R., Kleanthous, C., and Radford, S. E. (1999) Rapid folding with and without populated intermediates in the homologous four-helix proteins Im7 and Im9, *J. Mol. Biol. 286*, 1597−1608.
31. Linderstrøm-Lang, K. (1958) in *Symposium on Protein Structure* (Neuberger, A., Ed.) Methuen, London.
32. Pace, C. N. (1975) The stability of globular proteins, *CRC Crit. Rev. Biochem. 3*, 1−43.
33. Englander, S. W., and Kallenbach, N. R. (1984) Hydrogen exchange and structural dynamics of proteins and nucleic acids, *Q. Rev. Biophys. 16*, 521−655.
34. Huyghues-Despointes, B. M. P., Scholtz, J. M., and Pace, C. N. (1999) Protein conformational stabilities can be determined from hydrogen-exchange rates, *Nat. Struct. Biol. 6*, 910−912.
35. Grantcharova, V. P., and Baker, D. (1997) Folding dynamics of the src SH3 domain, *Biochemistry 36*, 15685−15692.
36. Hosszu, L. L., Baxter, N. J., Jackson, G. S., Power, A., Clarke, A. R., Waltho, J. P., Craven, C. J., and Collinge, J. (1999) Structural mobility of the human prion protein probed by backbone hydrogen exchange, *Nat. Struct. Biol. 6*, 740−743.
37. Nicholson, E. M., Mo, H., Prusiner, S. B., Cohen, F. E., and Marqusee, S. (2002) Differences between the prion protein and its homologue Doppel: a partially structured state with implications for scrapie formation, *J. Mol. Biol. 316*, 807−815.
38. Khorasanizadeh, S., Peters, I. D., and Roder, H. (1996) Evidence for a three-state model of protein folding from kinetic analysis of ubiquitin variants with altered core residues, *Nat. Struct. Biol. 3*, 193−205.
39. Park, S. H., O'Neil, K. T., and Roder, H. (1997) An early intermediate in the folding reaction of the B1 domain of protein G contains a nativelike core, *Biochemistry 36*, 14277−14283.
40. Kraulis, P. J. (1991) MOLSCRIPT: a program to produce both detailed and schematic plots of protein structure, *J. Appl. Crystallogr. 24*, 946−950.

BI0357412